Object-oriented classification and mapping of salt marsh vegetation using in situ radiometry and multi-seasonal, high resolution satellite remote sensing data

Object-oriented classification and mapping of salt marsh vegetation using *in situ* radiometry and multi-seasonal, high resolution satellite remote sensing data

Martha Gilmore*, Emily Wilson†, Daniel Civco†, James Hurd†, Sandy Prisloe†, Cary Chadwick†, & Nels Barrett‡
* Department of Earth and Environmental Sciences, Wesleyan University, 265 Church St., Middletown, CT, USA 06459, Email: mgilmore@wesleyan.edu
† Center for Land use Education and Research, Department of Natural Resources Management and Engineering, University of Connecticut, U-4087, Room 308, 1376 Storrs Road, Storrs, CT, 06269-4087, USA, Email: *firstname.lastname*@uconn.edu
‡ U.S. Department of Agriculture, Natural Resources Conservation Service, 344 Merrow Road, Suite A, Tolland CT, USA, 06084, Email: nels.barrett@ct.usda.gov

Abstract — The coastal marsh ecosystems around the Long Island Sound estuary are changing due to anthropogenic pressure, invasive species, habitat restoration and management, and sea level rise. It has become increasingly important to develop methods to characterize and classify marsh vegetation to monitor changes over time, understand the mechanisms of change, and develop baseline data to measure the efficacy of ongoing restoration and management programs. This study examines the effectiveness of using multitemporal satellite imagery and field spectral data to classify and map the common plant communities of the Ragged Rock Creek marsh, located near the mouth of the Connecticut River. The dominant marsh species, *Spartina patens*, *Phragmites australis* and *Typha* spp., have been found to be separable based on their individual spectral and structural characteristics and the phenological variability of each species. Classification methodology includes the segmentation of QuickBird multispectral imagery collected between 2004-2006 into image objects, which are then classified based on visible to near-infrared reflectance spectra collected in the field from 2004-2006 at the Ragged Rock Creek marsh. The field data are processed to create QuickBird band ratios, that are used to assign each image object as one of the dominant plant species found in the marsh. In addition, LIDAR data, collected on a single date in 2004, have been analyzed to determine average heights of dominant plants. These canopy height data are useful for discriminating among the marsh species, and contribute dramatically to the object-oriented classification of the QuickBird multispectral data. Collectively, these datasets and protocols provide a set of guidelines recommended for future remote sensing data collection in marsh inventory and analysis projects.

I. Introduction

Coastal wetlands are a critical component of the Long Island Sound ecosystem. However, over the past century, a significant amount of these wetlands has been lost due to development, filling and dredging, or damaged due to anthropogenic disturbance and modification. Global sea level rise is also likely to have a significant impact on the condition and health of coastal wetlands, particularly if the wetlands have no place to migrate due to dense coastal development. In addition to physical loss of marshes, the species composition of marsh communities is changing. *Spartina alterniflora* (salt cordgrass) and *Spartina patens* (salt marsh hay), once the dominant species of New England salt marshes, are being replaced by monocultures of the non-native genotype of *Phragmites australis* (Cav.) Trin. *ex* Steud (common reed) in Connecticut marshes [1]. With the mounting pressures on coastal wetland areas, it is becoming increasingly important to identify and inventory the current extent and condition of coastal marshes located on the Long Island Sound estuary, implement a cost effective way to track changes in the condition of wetlands over time, and monitor the effects of habitat restoration and management. The ultimate goal of this project is to provide protocols that can be used to classify multispectral data which are most available to land managers.

II. Data and Methods

A. Study Sites

Ragged Rock Creek Marsh is a 142 hectare brackish tidal marsh located on the western shore of the Connecticut River, approximately 2.5 km north of its confluence with Long Island Sound (Fig. 1). The vegetation at Ragged Rock Creek Marsh is typical of Connecticut's estuarine tidal marshes, where the pattern of growth is generally controlled by salinity, a function of tidal inundation and therefore elevation. In general, Ragged Rock Creek is characterized by a mosaic of brackish meadows and brackish reed marshes. Salt meadow cordgrass (*Spartina patens*) dominates the meadows in many areas of Ragged Rock with scattered occurrences of black grass (*Juncus gerardii*) and spike grass (*Distichlis spicata*). Smooth cordgrass (*Spartina alterniflora*) and occasionally tidalmarsh amaranth, (*Amaranthus cannabinus)* are characteristic plants of the low marsh, often found along the banks of the tidal creeks. The high marsh areas and upper border typically support dominant stands of narrow-leaved cattail (*Typha angustifolia*), hybrid cattail (*Typha x glauca*) and the non-native common reed (*Phragmites australis*). *P. australis* is common throughout the marsh often forming dense monotypic stands in the mid to high marsh. Additionally, its distribution is strongly correlated to the

mosquito ditches that exist throughout the marsh, a pattern that has been documented in other studies [2].

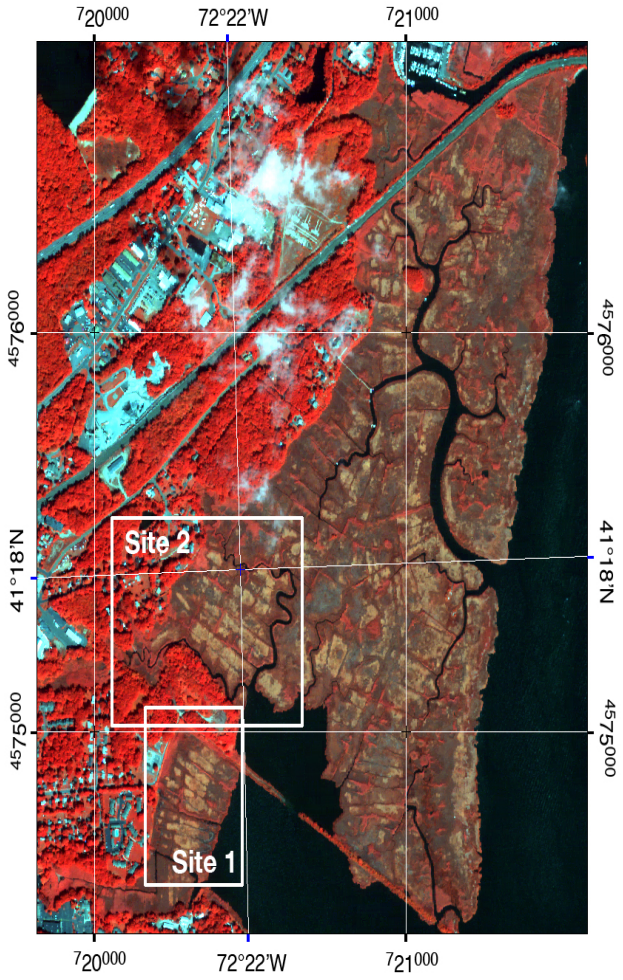

Fig. 1. QuickBird image of Ragged Rock Marsh in southern Connecticut

B. Data

Reflectance spectra were obtained using an ASD Fieldspec FR spectroradiometer (Analytical Spectral Devices, Boulder, CO) with a wavelength range of 350-2500 nm, a sampling interval of 1.4 nm between 350-1000 nm and 2 nm between 1000-2500 nm, and a spectral resolution of 3 nm between 350-1000 nm and 10 nm between 1000-2500 nm. The spectrometer is equipped with a 1 m long fiber optic sensor with a 25° field of view. Spectra were collected by positioning the fiber optic sensor ~nadir within 1 m of the species canopy by hand. Late in the season, the height of *Phragmites* prohibited a nadir view and canopy spectra were collected at an oblique angle. Individual spectral measurements were an average of five scans and each canopy was generally sampled 10 or more times. Reflectance spectra were normalized to a white Spectralon® (sintered Halon) panel. All spectra were collected between 10 am and 2 pm, except for 10/1/05, where the tides limited marsh access to the late afternoon (~4 pm).

To correlate better the field spectra to satellite data, individual field reflectance spectra were averaged over the four QuickBird band intervals to produce a simulated QuickBird band value (Fig. 2). The values for individual samples were averaged to attain a single reflectance value for each target and a standard deviation was calculated. From these data, five simple spectral indices were calculated: Band 2/Band 1, Band 4/Band 3, Band 3/Band 2, Band 4/Band 2 and the Normalized Difference Vegetation Index (NDVI = (Band 4 – Band 3)/(Band 4 + Band 3)).

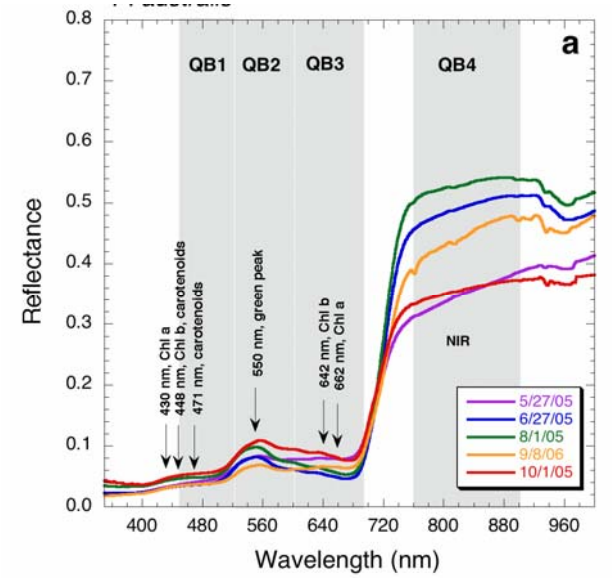

Fig. 2. Multitemporal spectral reflectance of *Phragmites australis*

A floristic inventory of the marsh was conducted throughout the summer of 2006, in large part to establish sets of training and validation data for image classification work. A set of 1,000 randomly distributed point locations within the marsh was generated. At each location, 4 m^2 quadrats were placed and plant community composition and species abundance were recorded. Field GPS coordinates for each sampling site were recorded using Trimble GeoExplorer3 GPS units and were post-processed to improve accuracy using Trimble GPS Pathfinder Office, or coordinates were recorded using Garmin Map 76CSx GPS coupled with a CSI-Wireless MBX-3S Differential Beacon Receiver for enhanced accuracy using real-time differential correction. Data collected at each sampling site included: species present, estimated percent cover for each species, height of dominant species, and sociability rank for each species based on its distribution (*e.g.*, tightly clustered in one area vs. distributed throughout) across the plot. Digital photographs also were taken at each site to document field conditions at the time the inventory was conducted. In total, 920 vegetation plots were recorded at Ragged Rock Creek; 875 were random plot locations and 45 were subjective plot locations selected by the field teams as unusual, rare or monotypic plant communities. Some plots were revisited during the growing season; only one data point

was maintained for each plot location resulting in a grand total of 894 field points.

Multitemporal, multispectral high resolution (2.44-meter at nadir) QuickBird satellite image data were acquired for a 100 km^2 area at the mouth of the Connecticut River (Fig 3.) from July 2003 through November 2006. The QuickBird multispectral sensor collects reflected radiation in the blue (450-520 nm), green (520-600 nm), red (630-690 nm) and near-infrared (760-900 nm) portions of the electromagnetic spectrum.

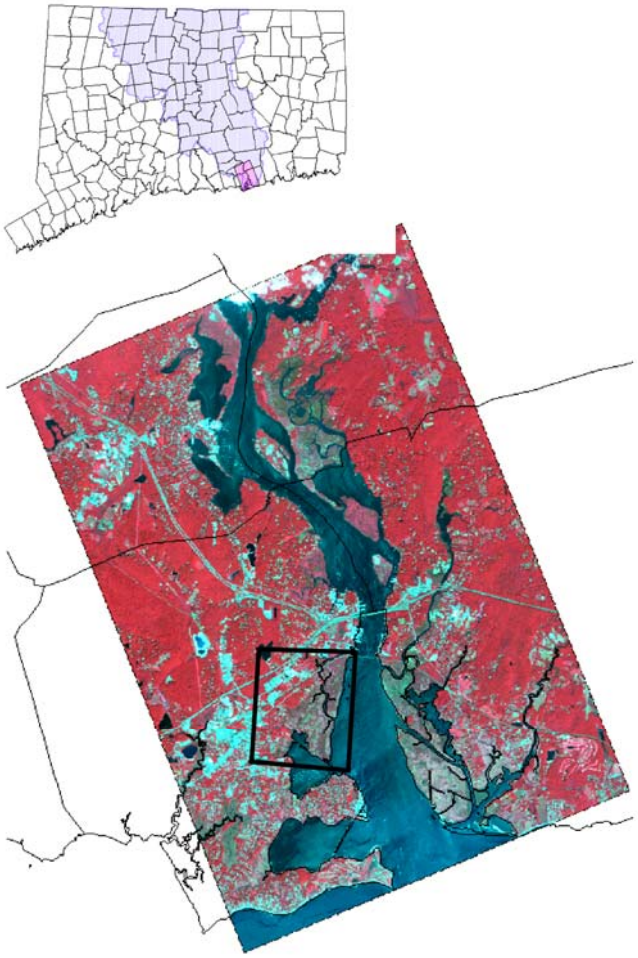

Fig. 3. Location of multiple QuickBird image acquisitions

Eleven QuickBird scenes were acquired during the late spring to early fall growing season over the four year period for the Lower Connecticut River Study area. While the intent was to collect multiple QuickBird scenes throughout a single growing season in order to incorporate seasonal changes within plant communities in the classification, due to weather and satellite competition, it took three years to capture imagery that was adequately distributed throughout the growing season Of the eleven scenes, five were selected to be used in the final classification based on image quality (lack of clouds and haze) and acquisition month and day, and importance as determined by field spectra data analysis. Selecting five images is consistent with *Key et al*. [3] who found that, when classifying tree species, there was a steady increase in classification accuracy as dates were added, up to six dates. Although the images spanned several growing seasons, the month and day of acquisition was considered more important than the year of acquisition because the monthly phenologic variability was observed to be much greater than inter-annual variability in the data set.

C. Classification

Of the five simple band ratios calculated from the field reflectance spectra, four were determined to be most useful in identifying at least one major plant community from all others on the radiometry rule graphs. The four band ratios (4/3, 4/2, 3/2, 2/1) were calculated for the five QuickBird images using image ratio models in ERDAS Imagine, resulting in 20 potential band ratio images to use in classification. The radiometry rules determined that 14 band ratio images could potentially be beneficial in classification by contributing to the separation of plant classes. The only raw QuickBird data applied to the classification was July 20, 2004 Near-IR band 4 in order to separate water from vegetated areas. A polygon of the Ragged Rock Creek marsh was used to further subset each band ratio image to eliminate variability from non-marsh features such as houses, trees and lawns.

eCognition (version 3.0, Definiens Imaging) an image segmentation and object-oriented classification software system, was used as the basis for QuickBird image classification. eCognition first segments images by grouping pixels into homogeneous regions and then applies fuzzy classification to image rules and/or training samples to produce a classification [4]. The band ratios listed in section II.B., a LiDAR data set with 0.9 meter spacings, and the four raw bands of the July 20, 2004 QuickBird image were added to eCognition. Each layer in the project is weighted to determine how much it contributes to segmentation, or the creation of boundaries that maximize heterogeneity between homogeneous objects. The segments are treated as units and each is classified as single entity. This is in contrast to per-pixel classifiers where each pixel is treated independently of all others, including its neighbors. In this case, thirteen of the fourteen image ratios had a weight of 0.5 on a scale of 0 to 1 and one ratio, the July 20, 2004 2/1 ratio had a weight of 0 because the July 20, 2004 Quickbird image was the only raw date of imagery included in the project. The blue, green and red bands of the July 20, 2004 QuickBird image had a weight of 0.8 and the NIR band had a weight of 1.0. The LiDAR had a weight of 1.0.

The relative size of each segment is determined by the scale parameter of the eCognition project. The scale parameter determines the maximum allowed heterogeneity between image objects making it related to segment size. Although multiple sizes of nesting segments are possible, trial and error revealed that one segment level was acceptable for this application. After trying many different scale parameters and assessing the variety of output segment sizes, a scale parameter of 20 was determined to be the optimum size to best mimic the marsh community in the QuickBird data.

Spectral information contributed 70% and spatial information contributed 30% to segment boundary determination.

The second step is classification where each segment is assigned to a class. The radiometry rules guided the writing of rules which eventually determined the classification result, by revealing which species in which band ratio were distinct from other species. The classification thresholds were determined using one-third of the field points (305) and built-in eCognition tools such as *Feature View*, which displays each segment, or object, in grayscale according to its value for the selected feature. For example, selecting the September 4/3 band ratio in feature view displays an image where dense vegetated features such as trees appear light or white, and segments representing non-vegetation are black. Other vegetated segments are colored in varying shades of gray. It is a valuable tool when selecting rule thresholds. One third of the field points (305 points) were randomly selected to help guide the classification. The remaining two thirds of the points were reserved for accuracy assessment.

D. Accuracy Assessment

The accuracy assessment determines the quality of information derived from remote sensing data [5] and indicates the sources of error. Two-thirds of the field points (n = 613) were utilized for accuracy assessment. Because GPS error could be as great as 2 meters, a 2 meter buffer was calculated for each point. A point was eliminated from the accuracy assessment if the buffer area included more than one class on the classified image. Of the 613 points available for accuracy assessment, 227 were eliminated due to the buffer criterion leaving 386 points. *Kappa* coefficients (KHAT) were calculated using the method of Congalton and Green [5].

III. Results

A. Phenology of major species

The shape of the reflectance spectra of each species (Fig. 4) is broadly similar, including the following absorptions typical of healthy photosynthesizing vascular plants: 430 nm (Chl *a*), 448 nm (Chl *b*, carotenoids), 471 nm (carotenoids), 642 nm (Chl *b*), 662 and 680 nm (Chl *a*), the green peak at 550 nm and strong reflectance in the NIR at ~800 nm. During the greenup phase of growth near the beginning of the growing season, each spectrum shows expected increases in the strength of the absorptions at ~450 nm and ~680 nm due to chlorophylls and carotenoids within the leaves and an increase in NIR reflectance due to leaf biomass. This trend continues in each species until the onset of senescence. Comparison of the spectra of individual species on each sampling date shows that the magnitude and shape of the spectra differ qualitatively, which is a function of each species' chemistry, biomass and phenological cycle.

To relate spectral variability to the QuickBird data, reflectance spectra of each species taken during both field seasons are reduced to QuickBird band ratios and plotted in Figure 5. The spectral behavior of the two sites is broadly consistent over the two growing seasons. Trends of NDVI and the 4/3 ratio mimic each other, with the 4/3 ratio providing greater separability amongst the individual points (Fig. 5a,b). All species show a rise in these indices at approximately day 160 (early June) corresponding with the green-up phase of plant growth and a decline in the indices corresponding to senescence. The behavior of the seasonal variation in each index varies with plant species. *S. patens* and *Phragmites* reach peak values at day 200 and *Typha* at day 170. *Typha* NDVI and 4/3 values are generally higher than the other species near the time of its peak (mid to late June), while *Phragmites* values exceed the other species in mid August through early September.

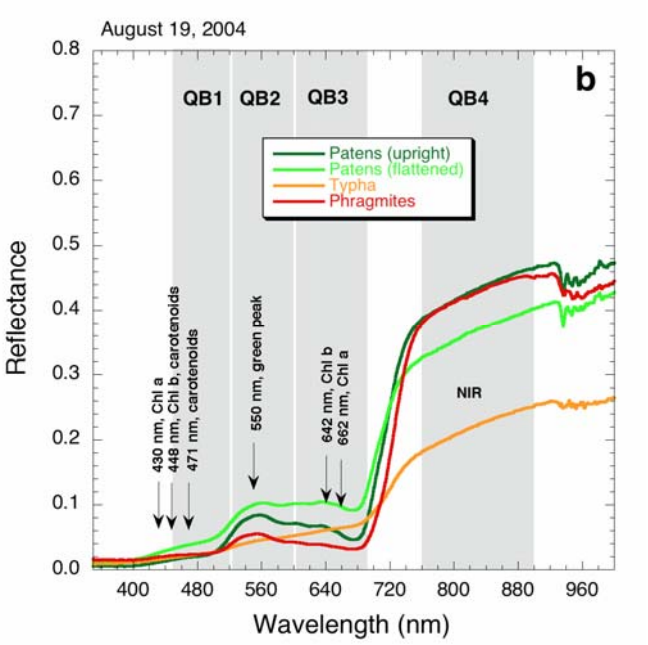

Fig. 4. Spectral reflectance of *S. patens*, *Typha* spp., and *P. australis* acquired through *in situ* radiometry, August 19, 2004.

The seasonal pattern of the QuickBird 2/1 ratio of *S. patens* is distinct from the other two species (Fig. 5c). Values of this ratio are similar for each species at the beginning of the season, but *S. patens* rises to a peak value ~ day 200. The absolute value for *S. patens* is twice that of *Typha* and *Phragmites* from early June through early August.

The general seasonal pattern of the QuickBird 3/2 ratio for all species shows an initial decline from day 140 to ~ day 180 and then an increase (Fig. 5d). *S. patens* values in this index are lower than the other two species over days 165 to 225 (mid June – early August). *Typha* values exceed those of the other species from mid-July onward.

The general seasonal pattern of the QuickBird 4/2 ratio for all species shows an increase in the middle portion of the growing season and decline at the end (Fig. 5e). *S. patens* values in this index are consistently lower than the other two species throughout the year. Values for *Typha spp.* are higher than and separable from the other two species in mid to late June. Values for *P. australis* are higher than and separable from the other two species in late August – early September.

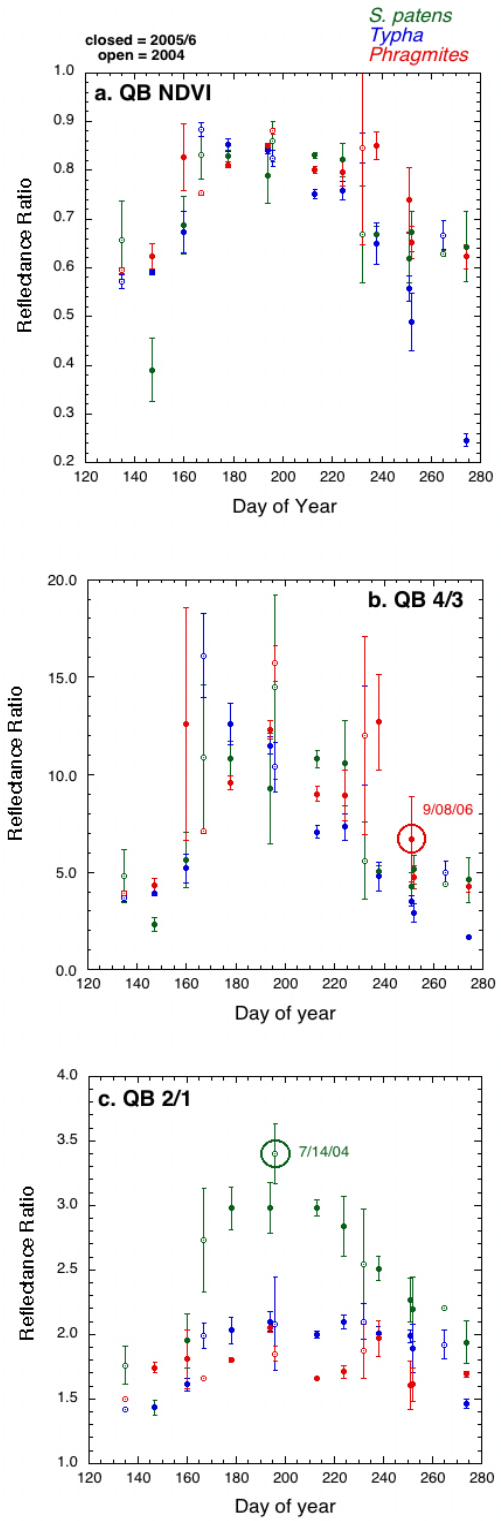

Fig. 5. Multitemporal QuickBird (a) NDVI, (b) band 4/3 ratio, (c) band 2/1 ratio, (d) band 3/2 ratio, and (e) band 4/2 ratio

Of the five simple band ratios calculated from the field reflectance spectra, four were determined to be most useful in identifying at least one major plant community: for *P. australis*, the 4/3 ratio on September 8, 2006, for *S. patens*, the 2/1 ratio on July 14, 2004, and for *Typha spp*., the 3/2 ratio on August 12, 2005 and the 4/2 ratio on June 15, 2004. These dates both show the greatest spectral separability between individual species and best correspond with the dates of the QuickBird images available for classification.

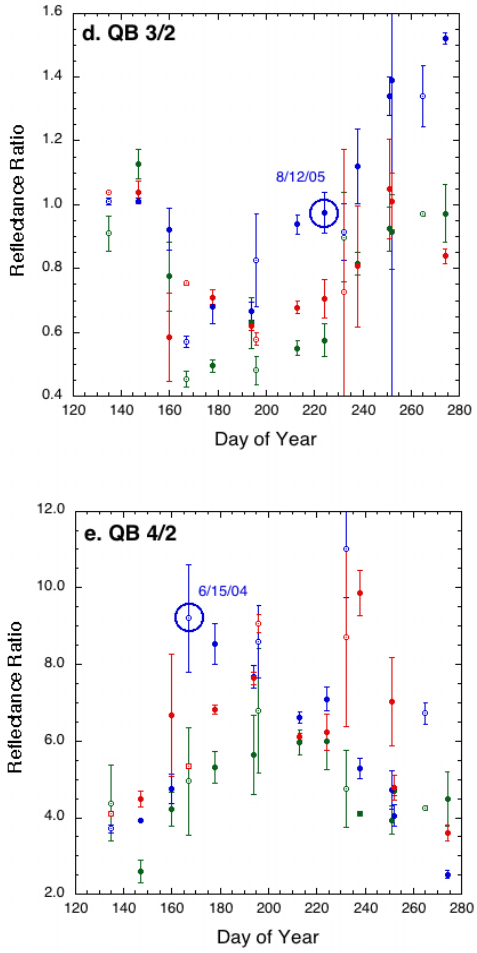

B. QuickBird Classification

QuickBird classification results are displayed in Fig. 6. Qualitatively, the classification identifies contiguous areas of *P. australis*, *Typha spp.*, and *S. patens*. The distribution of these classes is broadly consistent with field observations, for example, the correlation of *P. australis* and anticorrelation of *S. patens* with creeks and ditches. An accuracy assessment of the classification results was performed where each validation point is assigned to dominant classes. The overall accuracy was 66.8% with a *kappa* coefficient of 0.56. *P. australis* had the highest user's accuracy (87.0%) and a high producer's accuracy (76.9%). *Typha spp.* had the lowest user's accuracy (59.1%) but the highest producer's accuracy (88.3%) indicating an over-classification of other/mixed reference points as *Typha spp.* *S. patens* had a similar over-classification with 32 points being classified as *S. patens* but being labeled other/mix on the reference dataset. The result was 62% user's accuracy for *S. patens* and a 79.2% producer's accuracy. The over-classification of *Typha spp.*

and *S. patens* is more likely to be an artifact of the reference dataset and the assignment of class dominance to a complex field point dataset than a true inability to classify.

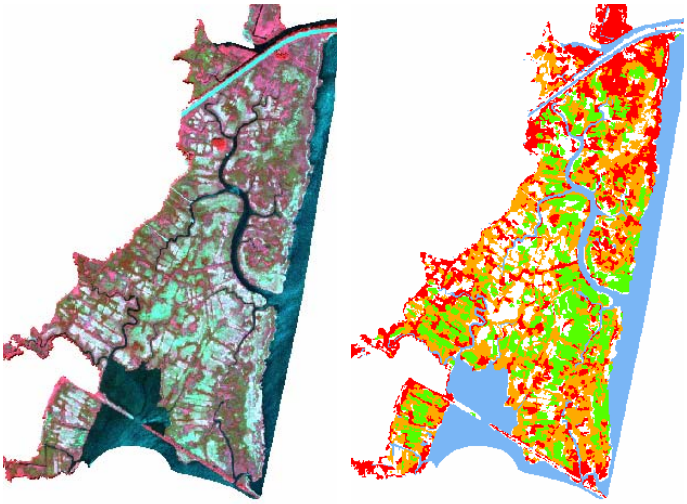

Fig. 6. QuickBird image (Bands 4, 2, 1) and classification results (red=*Phragmites australis*, green=*Spartina patens*; orange=*Typha* spp.)

Because of the difficulty in assigning continuous and complex floristic data to one single class, the accuracy table was re-calculated where the validation data are defined by the **presence** of the named species. This results in an increase in overall accuracy to 82.9% (*kappa* coefficient = 0.77) as well as producer's and user's accuracies in each category. The User's accuracy for the three species classes improved dramatically. Seven of the nine points classified as *P. australis* but labeled other/mixed, contained some *P. australis*. Twenty-two of the 42 points classified as *Typha spp*. but labeled as other/mixed, contained *Typha spp.* and 25 of the 32 points classified as *S. patens* but labeled other/mixed contained *S. patens*. The greatest change is the improvement of commission errors for *S. patens*, which we suggest results from its distribution as understory in many of the validation quadrats. Although all three species saw a slight improvement in producer's accuracy with *P. australis* going from 76.9% to 82.7%, *Typha spp.* changing from 88.3% to 92.9% and *S. patens* changing from 79.2% to 85.9%, the greatest improvement in producer's accuracy occurred in the other/mix class. In this presence/absence accuracy table, reference points were moved out of the other/mix class and into the appropriate species class, leaving the other/mix class containing points that did not contain any *P. australis, Typha spp.* or *S. patens*. In other words, the other/mix class more accurately represents other and mixed species.

III. Discussion and Conclusions

The spectral characteristics of vegetation are due to in leaf pigments, plant structure (biomass and canopy architecture and cover) and plant health throughout the phenological cycle. The variability observed in individual reflectance spectra is replicated when these spectra are resampled to QuickBird bands. Much of the spectral variability in the resampled data can be attributed to expected increases in plant pigments and biomass during the green up phase of plant growth, and the decline of these parameters during senescence. The magnitude and rate of these changes is found to differ in individual species allowing their spectral discrimination.

Many studies have shown a correlation between the near-infrared reflectance of vegetation and biomass. This effect is seen in the resampled data where *P. australis* and *Typha spp*., both dense monocultures ≥ 2 meters high, have higher NDVI, 4/3 and 4/2 values throughout the growing season than the low growing *S. patens* (Figs. 5a, b, e). NIR index values peak for *Typha spp*. in the mid - late June, corresponding to field observations of peak plant heights of 6 to 7 feet, full development of flowers and wholly green leaves. *P. australis* displays peak NIR index values in mid August to early September correlating to peak plant heights of up tp four meters and the development of flowers. Additionally, by late August, *Typha* leaves are mostly brown, exacerbating the NIR distinction between the two species on this date. The differences in the timing of peak biomass between *Typha* and *P. australis* were used to discriminate between these two species in the classification. The late season peak in NIR reflectance for *P. australis* [6,7,8] and its distinction from Typha [9] have been noted in other marshes.

Some of the variability in the spectral indices can be correlated to genetic differences in pigment concentrations between the three species. The green:blue of S. patens is dramatically higher than that of *P. australis* or *Typha* from mid June through late August (Fig. 5c). We attribute this to inherent differences in the amount of chlorophyll *b* and carotenoids in these species, both of which absorb in the blue portion of the spectrum (Fig. 4). This effect can be seen in the field, where both *P. australis* and *Typha* leaves are observed to have a slight bluish hue. The peak in the 2:1 index for *S. patens* in mid July corresponds to maximum pigment concentration at this time of year. This is also the time of peak biomass of this species as recorded in the NIR ratios, but, in general, the NIR indices for *S. patens* cannot be separated as well from the other species.

Typha also records seasonal changes in pigment concentrations that were useful for classification. Values for red:green are higher for *Typha* than the other species in early August (Fig. 4d) likely due to a reduction in leaf chlorophyll pigments during senescence in this species at this time. The timing of *Typha* senescence is also recorded in the NIR and both the 3:2 and 4:2 indices were utilized to distinguish *Typha* in the classification.

The resampled spectral data generate the following set of spectral rules that may be applicable to the distinction of P. australis, *Typha* and *S. patens* communities: 1) *P. australis* is best distinguished by its high NIR response late in the growing season due to its high biomass especially with respect to the other species, 2) *Typha* is best distinguished by NIR response in June and high red: green response in August

which correspond to peak biomass and senescence, respectively, and 3) *S. patens* is best distinguished by pigment differences that result in a unique green:blue throughout the growing season, peaking in July. These indices suggest that multispectral data such as QuickBird is adequate to remotely measure and distinguish the phenological characteristics of these species. The data further suggest that if these phenological relationships hold from year to year, these rules can be applied to single date multispectral data to look for particular species. For example, our observations lead us to recommend acquisition of color infrared or four band satellite data during late August to early September to facilitate detection of *P. australis*.

The phenological trends seen here can vary as a function of plant vigor, which may depend on changes in salinity, weather, predation or disturbance. That these trends are consistent over two years at two separate areas of Ragged Rock Creek Marsh suggests that these rules may have broader spatial and temporal application, but are perhaps best limited to regions of consistent climate.

REFERENCES

[1] Warren, R.S., Fell, P.E., Grimsby, J.L., Buck, E.L., Rilling, G.C., & Fertik, R.A. (2001). Rates, patterns, and impacts of *Phragmites australis* expansion and effects of experimental *Phragmites* control on vegetation, macroinvertebrates, and fish within tidelands of the lower Connecticut River. *Estuaries, 24*, 90-107

[2] Bart, D., Burdick, D., Chambers, R., & Hartman, J. M. (2006). Human facilitation of Phragmites australis invasions in tidal marshes: A review and synthesis. Wetlands Ecology and Management, 14, 53-65.

[3] Key, T., Warner, T.A., McGraw, J.B., Fajvan, M.A. (2001). A comparison of multispectral and multitemporal information in high spatial resolution imagery for classification of individual tree species in a temperate hardwood forest. Remote Sensing of Environment, 75:100-112.

[4} Benz, U.C., Hofmann, P., Willhauck, G., Lingenfelder, I. & Heynen, M. (2004). Multi-resolution, object-oriented fuzzy analysis of remote sensing data for GIS-ready information. Photogrammetry and Remote Sensing, 58, 239-258.

[5] Congalton, R.G. & Green, K. (1999). Assessing the Accuracy of Remotely Sensed Data: Principles and Practices. Lewis Publishers, Boca Raton, FL.

[6] Artigas, F.J., & Yang, J.S. (2005). Hyperspectral remote sensing of marsh species and plant vigour gradient in the New Jersey Meadowlands. Int. J. Remote Sensing, 26, 5209-5220.

[7] Artigas, F.J., & Yang, J.S. (2006). Spectral discrimination of marsh vegetation types in the New Jersey Meadowlands, USA. Wetlands, 26, 271-277.

[8] Gao, Z.G., & Zhang, L.Q. (2006). Multi-seasonal spectral characteristics analysis of coastal salt marsh vegetation in Shanghai, China. *Estuarine, Coastal Shelf Science, 69*, 217-224.

[9] Laba, M., Tsai, F., Ogurcak, D., Smith, S., & Richmond, M.E. (2005) Field determination of optimal dates for the discrimination of invasive wetland plant species using derivative spectral analysis. *Photogrammetric Engineering & Remote Sensing, 71*, 603-611.